The TBX3 gene, mutated in Ulnar-Mammary syndrome, promotes growth of mammary epithelial cells independently of ARF and p53.

Cell Tissue Res (2007) 328:301–316
DOI 10.1007/s00441-006-0364-4

REGULAR ARTICLE

TBX3, the gene mutated in ulnar-mammary syndrome, promotes growth of mammary epithelial cells via repression of *p19ARF*, independently of *p53*

Natalia Platonova · Maddalena Scotti · Polina Babich · Gloria Bertoli · Elena Mento · Vasco Meneghini · Aliana Egeo · Ileana Zucchi · Giorgio R. Merlo

Received: 5 August 2006 / Accepted: 27 November 2006 / Published online: 30 January 2007

Abstract *TBX3*, the gene mutated in ulnar-mammary syndrome (UMS), is involved in the production of a transcription factor of the T-box family, known to inhibit transcription from the *p14ARF* (*p19ARF* in mouse) promoter in fibroblasts and to contribute to cell immortalization. One of the main features of the UMS phenotype is the severe hypoplasia of the breast, associated with haploinsufficiency of the *TBX3* gene product. In mice homozygous for the targeted disruption of *Tbx3*, the mammary glands (MGs) are nearly absent from early stages of embryogenesis, whereas in heterozygous adults, the MGs show reduced ductal branching. All these data strongly suggest a specific role of *TBX3* in promoting the growth of mammary epithelial cells (MECs), although direct evidence of this is lacking. Here, we provide data showing the growth-promoting function of *Tbx3* in several models of MECs, in association with its ability to repress the *ARF* promoter. However, no effect of *Tbx3* on cell differentiation or apoptosis has been observed. The growth promoting function also entails the down-regulation of $p21^{CIP1/WAF}$ and an increase in cyclin D1 but is independent of p53 and Mdm2 cell-cycle regulatory proteins, as *p53*-null MECs show similar growth responses associated with the up- or down-regulation of *Tbx3*. This is the first direct evidence that the level of *Tbx3* expression positively controls the proliferation of MECs via pathways alternative to Mdm2-p53.

Keywords Tbx3 · p19ARF · p53 · Mammary cells · Proliferation · Ulnar-mammary syndrome · Cell culture (Mouse)

G.R.M. is a recipient of a Career Award from Fondazione Telethon, Italy (S99003) and is supported by the Italian Ministry of Foreign Affairs (10-RB18), Fondazione Cariplo (S00083FCRA), Fondazione SanPaolo (99003CSPC) and Istituto Superiore di Sanità. N.P. is in receipt of a NATO-CNR Advanced Fellowship (N215-36S). I.Z. is supported by AIRC Italy (N. 115), Fondazione Cariplo (2003/1656), Italy-USA Project on Cancer Pharmacogenomics (N. 527/B-B7) and Italian Ministry of University and Research-FIRB Internazionale (RBIN04CBSM_000). The work of I.Z. and G.R.M. is also financed by a grant from Fondazione Telethon (GGP04247).

N. Platonova · P. Babich · V. Meneghini · A. Egeo · G. R. Merlo (✉)
Dulbecco Telethon Institute/CNR-ITB,
Via F.lli Cervi 93 Segrate,
Milano 20090, Italy
e-mail: gmerlo@dti.telethon.it

M. Scotti · G. Bertoli · E. Mento · I. Zucchi
Istituto Tecnologie Biomediche CNR,
Via F.lli Cervi 93 Segrate,
Milano 20090, Italy

P. Babich
Research Institute of Experimental Medicine,
St. Petersburg, Russia

Introduction

The mammary gland (MG) undergoes a complex series of changes from intrauterine life to senescence. The various stages of MG development include embryonic, prepubertal and pubertal phases, plus pregnancy, lactation and involution (Daniel and Smith 1999). Development of the MG is initiated in early mammalian embryos and undergoes a complex morphogenesis that results in the formation of primary ducts and the end-bud (Hennighausen and Robinson 1998; Veltmaat et al. 2003; Rowley et al. 2004). Growth and morphogenesis continue mainly at puberty under the influence of hormones and entail massive proliferation of multipotent cells, duct extension and branching. Finally, the

organization of a functionally differentiated and mature MG occurs cyclically with each pregnancy, followed by the lactation and involution phases. Embryonic and pre-pubertal growth of the MG is referred to as being hormone independent, whereas pubertal growth and pregnancy-dependent maturation require specific sexual hormones (Visvader and Lindeman 2003; Groner 2002).

During all these steps, signals between the epithelium and the surrounding mesenchyme and stroma are critical; in particular, during embryonic growth, several molecules (such as members of the Wnt and fibroblast growth factor families) convey signals that induce placode formation and thickening, followed by duct elongation and primitive branching (Hennighausen and Robinson 1998; Rowley et al. 2004). Together with the expansion of the mesodermal component of the MG, these events collectively result in the morphogenesis of the gland. Transcription factors and co-factors (such as members of the LEF, Msx and Hox families) present in the epithelial cells mediate the response to extracellular signals by regulating the transcription of target genes (for reviews, see Rowley et al. 2004; Visvader and Lindeman 2003; Groner 2002; Coletta et al. 2004). Little is known about transcription factors controlling the intrinsic growth potential of mammary epithelial cells (MECs).

The highly regulated process of growth, morphogenesis and differentiation of the MG is impaired in patients with ulnar-mammary syndrome (UMS, OMIM 181450). UMS is characterized by upper limb skeletal malformations, severe hypoplasia of the breast and other apocrine glands, and hair and genital defects. In UMS patients, one allelic copy of the *TBX3* gene is mutated, often resulting in the synthesis of a truncated non-functional protein and insufficient level of wild-type (WT) TBX3 protein (a transcription factor of the T-box family), a situation known as haploinsufficiency (Bamshad et al. 1997, 1999; Meneghini et al. 2006). The loss of one functional *TBX3* allele in UMS patients results in a severe congenital reduction or absence of the epithelial component of the MG. Thus, the precise level of *TBX3* gene expression and, consequently, the expression of its transcriptional targets appear to be critical for the control of the proliferation of mammary epithelial cells in vivo.

Germ-line and somatic inactivation of *Tbx3* in the mouse has been achieved (Davenport et al. 2003). Homozygous animals show UMS-related defects in a severe form and the mammary buds are absent by E13 and all subsequent stages, as evidenced by lack of expression of the early markers *Wnt10b* and *Lef1* (Davenport et al. 2003), whereas heterozygous appear to be normal. This outcome might have been expected based on the phenotype of "knock-out" mice for other *Tbx* genes, e.g. for *Tbx4* (Packham and Brook 2003; Naiche and Papaioannou 2003). Regrettably, *Tbx3*−/− embryos do not survive past E15-E16 and thus are of little use in the examination of mammary growth and histological organization as a consequence of *Tbx3* inactivation. Recently, Jerome-Majewska and collaborators (2005) have carried out a detailed analysis of the MG of *Tbx3*+/− females and report reduced branching of the ductal tree. It is still unclear whether the reduced branching is a direct consequence of the loss of one *Tbx3* alleles, in other words whether a cell-autonomous property is directly regulated by the level of *Tbx3* expression in MECs.

T-domain-containing genes (*Tbx*) are members of a highly conserved family of transcription factors that share a common DNA binding (T) domain (Papaioannou and Silver 1998; Smith 1999), which is essential for sequence-specific DNA binding and transcription activation or repression of target genes (Papaioannou and Silver 1998; Smith 1999; He et al. 1999; Wilson and Conlon 2002; Paxton et al. 2002; Butz et al. 2004). Some target genes have been identified (Tada and Smith 2001; Lingbeek et al. 2002), but not in MECs, the main cellular target in the UMS phenotype; in these cells, *Tbx3* transcription regulation is likely to be the result of cell-type-specific DNA binding and expression of the target genes. In non-mammary cells *TBX3* has been shown to repress the transcription of *ARF* potently (*p14ARF* in human, *p19ARF* in mouse; Lingbeek et al. 2002; Carlson et al. 2001; Brummelkamp et al. 2002), a positive regulator of the p53 pathway and also known as cyclin-dependent kinase inhibitor 2A (CDKN2A). The repression of *p14ARF* by TBX3 leads to cell immortalization of neuronal and embryonic fibroblasts (EF) (Carlson et al. 2001; Brummelkamp et al. 2002), an indication that the *p14ARF* gene might lie genetically downstream of *TBX3* in these cells.

As mutations in the *TBX3* gene cause the breast hypoplasia seen in UMS, and as *Tbx3* expression is found predominantly in the epithelial component of the embryonic mammary bud and the postnatal MG (Davenport et al. 2003; Jerome-Majewska et al. 2005; Chapman et al. 1996), we might logically expect that *Tbx3* has a positive role in the regulation of MECs growth, possibly by repressing *p19ARF*. In support of this hypothesis, the over-expression of *Tbx3* in mouse EFs and other non-epithelial cells leads to the onset of indefinite proliferation (Carlson et al. 2001; Brummelkamp et al. 2002). However, *TBX3* gene function should best be assessed in MECs, because the cell-type specificity of transcription regulation is likely to be co-determined by cell-type restricted co-factors (Tada and Smith 2001). This notion is particularly relevant since *Tbx3* and *Tbx2*, unlike other T-domain proteins, are known to be transcriptional repressors (Carreira et al. 1998; He et al. 1999; Carlson et al. 2001).

No data are available for MECs, the main cellular targets of *TBX3* mutations in vivo. Furthermore, little is known

about the *Tbx3* expression profile during postnatal MG growth and functional differentiation or about whether Tbx3 can repress *p19ARF* and act through a p53-dependent or p53-independent pathway of cell-cycle regulation. In the present study, we have addressed the cellular functions of *TBX3* by using the immortalized non-tumorigenic HC11 MECs that lack WT p53 as our main in vitro model (Danielson et al. 1984). These cells can partially differentiate in vitro, as they synthesize milk proteins following lactogenic hormone induction (Ball et al. 1988), a feature used in previous studies in which growth-promoting and inhibitory genes have been found to interfere with differentiation (Merlo et al. 1996). HC11 cells have the additional property to undergo apoptosis under specific serum-/growth-factor-deprivation conditions, reminiscent of the events occurring during the post-weaning involution of MGs (Merlo et al. 1995). Here, we show that *TBX3/Tbx3* regulates the growth of several MEC lines independently of *p53*, whereas the differentiation and apoptotic properties of these cells remain unchanged. TBX3 can repress *p19ARF* expression at the promoter level regardless of the *p53*. Exogenous expression of *TBX3* results in the reduced expression of the CDK inhibitor $p21^{CIP1/WAF}$, whereas the expression of *Mdm2* remains unaffected. We propose that *TBX3*-dependent growth promotion in MECs occurs via *p19ARF* and $p21^{CIP1/WAF}$, but independently of the Mdm2-p53 pathway.

Materials and methods

Expression and reporter vectors

The haemagglutinin (HA)-epitope-tagged *TBX3* expression vector (based on pCS2+) was provided by Drs. Hurlin and Ota (Carlson et al. 2001). This vector, which lacks a suitable selectable marker, was used solely in transient transfection experiments in COS7 and HC11 cells. For transfection and selection of clones, the HA-*TBX3* cDNA was subcloned into the *Bam*HI/*Sna*BI sites of the pBabe-puro vector (Morgenstern and Land 1990), carrying the puromycin-resistence selectable marker. The *p14ARF* luciferase-reporter construct was provided by Dr. M. Lingbeek (Lingbeek et al. 2002) and was used to assay for *TBX3*-dependent repression in MECs by transient transfection. The vector contains the −19/+54 region of the *p14ARF* promoter introduced into the pGL3-basic vector (Promega).

Cell cultures and treatments

HC11 mouse MECs (provided by Dr. N. Hynes, FMI, Basel) were maintained at 37°C/5% CO_2, in growth medium (GM) composed of RPMI-1640, 8% heat-inactivated fetal calf serum (FCS), 5 μg/ml insulin (Sigma) and 10 ng/ml murine epidermal growth factor (EGF; Sigma), glutamine and gentamycin (Merlo et al. 1994). For the differentiation assay, confluent cultures of HC11 cells were incubated in induction (DIP) medium containing RPMI1640, 8% FCS, 1 μM dexamethasone, 5 μg/ml ovine prolactin (Sigma) and 5 μg/ml insulin. Reduced medium contained RPMI-1640, 1% heat-inactivated FCS, 5 μg/ml insulin, glutamine and gentamycin. Serum-free medium (SFM) was prepared by adding 2% bovine serum albumin (BSA; Sigma) to RPMI. NulliB cells were derived from *p53*−/− mice (provided by Dr. D. Medina, Baylor College of Medicine, Houston, Tex.). These cells were maintained in RPMI, 2% FCS, 10 μg/ml insulin and 5 ng/ml EGF, glutamine and penicillin-streptomycin. LA7 and 106A10 rat MECs were cultured in DMEM, 10% FCS, insulin and hydrocortisone (50 ng/ml each) and penicillin-streptomycin. For the differentiation assay, confluent cultures of LA7 and 106A10 cells were exposed to 2% dimethyl sulphoxide (DMSO; Dulbecco et al. 1980). MDA435 and MCF7 breast cancer cells were maintained in DMEM with 10% FBS penicillin-streptomycin.

For depletion of the endogenous *TBX3/Tbx3*, we used four 21-nucleotide antisense oligonucleotides (AS oligos), three designed from the *Tbx3*-coding region, and one from the 3′-untranslated region (sequences provided in Tables 1, 2).

Table 1 Reverse transcription/polymerase chain reaction (PCR) and real-time quantitative PCR primers

Primer sequence	Annealing temperature in °C	Product size in bp
Mouse *Tbx3* 5′-TTGCAAAGGGTTTTCGAGAC 5′-GTTGGATGTCCCCACGAT	60	191
Human *TBX3* 5′-GCAGCTTTCAACTGCTTCG 5′-CCTCGCTGGGACATAAATCT	59	88
Mouse *p19ARF* 5′-CCCACTCCAAGAGAGGGTTT 5′-TCTGCACCGTAGTTGAGCAG	55	199
Mouse *mdm2* 5′-AGGGCACGAGCTCTCAGAT 5′-GAAGCCAGTTCTCACGAAGG	60	200
Mouse $p21^{CIP1/WAF}$ 5′-GGACAAGAGGCCCAGTACTTC 5′-TCTGCGCTTGGAGTGATAGA	58	187
Mouse *β-casein* 5′-GTTCAGGCTTTTCCTCAGAC 5′-CCATGGGTCGAATTCAAATG	60	393
Mouse *cyclin D1* 5′-GAGATTGTGCCATCCATGC 5′-CTCTTCGCACTTCTGCTCCT	55	75
Mouse *GAPDH* 5′-TGTATGCAGGGATGATGTTC 5′-TGTCAGCAATGCATCCTGCA	61	190

For chosing the appropriate sequences, we avoided regions of *Tbx3* mRNA likely to be involved in the formation of intra-molecular base pairing and secondary structures or regions partially conserved between T-box genes. Dependent on the employed cell line (murine/human), species-specific AS oligos were used. Sequences were verified by BLAST searches. Four control sense oligonucleotides (S oligos) were designed complementary to the AS oligos. For *p19ARF*, we used two 21-nucleotide AS oligos corresponding to sequences of the alternative-spliced exon 1β of the *INK4a/ARF* locus (see Tables 1, 2).

Oligomers were added three times a day for 3 days directly to the culture medium onto newly plated adherent cells (<20% confluency) at a total concentration of 0.25 mg/ml/day (Zucchi et al. 1998, 1999). To verify the down-regulation by AS oligos, total RNA was extracted from cells growing for 72 h and the relative abundance was determined by real-time quantitative polymerase chain reaction (qPCR, see below).

For the monolayer cell proliferation assay, cells were seeded in 96-wells clusters at the starting density of 5,000 cells/well. After the cells were attached, the first point (time 0) was taken, the subsequent points being taken 24, 48 and 72 h later. The number of viable cells was determined with the Cell Proliferation Kit I (MTT, Roche) according to manufacturer's instructions. Measurements were performed on triplicate points in an enzyme-linked immunosorbent assay reader at a wavelength of 600 nm and standard deviations were determined.

Programmed cell death was induced in MECs as described (Merlo et al. 1996). Briefly, cells were plated on chamber slides in GM. At confluence, cells were treated with SFM or with SFM plus EGF (10 ng/ml) for 48 h and then analysed. Two methods were used. For direct examination and counting, cells were fixed in 2% paraformaldehyde for 10 min, rinsed and stained with a solution containing 6′-diamidino-2-phenylindole (DAPI, 1:2,000), 0.1% Triton X-100, 0.1% Na citrate and 20 μg/ml RNaseA. Nuclei with morphological features of apoptosis were identified and counted. Alternatively, a flow-cytometric apoptotic assay was used to detect Annexin V-positive cells, corresponding to early apoptotic cells (Koopman et al. 1994), by using FACScan equipment (Becton-Dickinson), with Ex=488 nm, Em=530 nm. The assay was followed by the Annexin V-fluorescein isothiocyanate (FITC) Apoptosis Detection kit (MBL) according to the manufacturer's protocol. In this assay, Annexin V-negative and propidium iodide (PI)-positive signals corresponded to nuclear debris, Annexin V-positive and PI-positive signals corresponded to late apoptotic cells, Annexin V-negative and PI-negative signals corresponded to live cells and Annexin V-positive and PI-negative signals corresponded to early apoptotic cells. The experiments were repeated twice and standard deviations were calculated.

Table 2 Antisense (*AS*) oligonucleotides used

Oligonucleotide type	Sequence
AS *mouse Tbx3*	1. 5′ ACTTTAAACGGAGGGAACATT
	2. 5′ TTTGTGGAAAGTGACGACTTT
	3. 5′ GCAAAGGGATTGTTGTCTATT
	4. 5′ ATAATGGGACTTCCGTTGTTT
AS *human TBX3*	1. 5′ ACTTTAAATGGAGGAAACATT
	2. 5′ TTTGTGGAAAGTGACGACTTT
	3. 5′ GCAAAAGGGTTGTTGTCTATT
AS *p19ARF*	1. 5′ACAGTGACCAAGAACCTGCGA
	2. 5′TTCACGAAAGCCAGAGCGCAG

Transfection and reporter assays

For transient transfection, cells were transfected for 48 h with pCS2+HA-*TBX3* plasmid by using Lipofectamine-2000 (Invitrogen), according to the manufacturer's instructions. Transfected cells were either immunostained with anti-HA antibody (Y11, Santa Cruz Biotechnology) or used to prepare total protein lysates for Western blot analysis with the same antibody.

For the generation of cell lines expressing exogenous HA-*TBX3*, HC11 cells were seeded in duplicate in 35-mm dishes at a density of 2×10^5 cells per dish; 24 h later, cells were transfected with 4 μg HA-*TBX3*-pBabe-puro plasmid by using Lipofectamine-2000 and, after an additional 48 h, the cells were trypsinized, replated and cultured in GM containing puromycin (2.5 μg/ml) for 10–14 days before individual clones were picked and further propagated. The resulting clones were tested for the presence of HA-TBX3 protein by Western blot analysis and by immunostaining with anti HA-antibody.

For the reporter assay, transfections were carried out with Lipofectamine-2000, with 4 μg of the (−19/+54) *p14ARF*-luciferase reporter plasmid, 5 μg of the pCS2+HA-*TBX3* expression plasmid (or an equal amount of empty plasmid, as control) and 400 ng of a CMV-βgal plasmid to normalize for transfection efficiency. Prior to transfection, cells were plated in 6-well cluster dishes at a density 4×10^5 cells per well, in duplicates. Cells were cultured for 48 h and then lysed and assayed for promoter activity with the Luciferase Assay System (Promega). Luminescence values were normalized for β-gal activity levels and for total protein concentration in the lysates. Experiments were repeated three times.

Western blot and immunofluorescence analyses

For Western blot analyses, total proteins were extracted with RIPPA lysis buffer containing 150 mM NaCl, 50 mM

TRIS-HCl (pH 8.0), 1% NP40, 0.1% SDS, 1 mM phenylmethane sulphonyl-fluoride and 1:1,000 "protease cocktail inhibitor" (Sigma) for 15 min on ice, followed by sonication (2–3 W, 20 s). After centrifugation, the cleared lysates were resolved on 10% SDS-polyacrylamide gels, transferred to polyvinylidene fluoride membranes (Hybond, Amersham) and developed by using standard electrochemiluminescent procedures (Amersham). Primary antibodies were: rabbit anti-HA (Y11, Santa Cruz Biotechnology) used at a dilution of 1:200; rabbit anti-mouse milk proteins (from Dr. Hynes, FMI Basel) at 1:300; rabbit anti-p19 (Abcam) at 1:500. For the detection of milk proteins, 5% BSA was used as a blocking agent. Secondary antibody was peroxidase-conjugated goat anti-rabbit (Amersham) at 1:8,000.

For immunostaining, cells were plated on glass chamber slides (BD, Falcon) in GM, incubated for 24 h, fixed in methanol/acetic acid (3:1) for 5 min and rinsed with phosphate-buffered saline (PBS). After permeabilization with 0.5% Triton X-100, cells were incubated with 10% goat serum and then with anti-HA antibody (1:200) overnight at 4°C. As the secondary antibody, FITC-conjugated anti-rabbit antibody was used (1:100). Nuclei were counterstained with DAPI (1:2,000).

RNA extraction, cDNA synthesis and real-time qPCR

Cells or MG tissues were harvested in TriPure Isolation Reagent (Invitrogen) and total RNA was purified according to the manufacturer's instructions. RNA was quantified by using a NanoDrop Spectrophotometer ND1000. Total RNA (1 μg) was reverse-transcribed at 42°C for 50 min with random hexamers and SuperScriptII Reverse Transcriptase (Invitrogen). Relative cDNA abundance was measured by qPCR with a LightCycler 1.5 (Roche). Reactions were set up with the Fast Start DNA Master SYBR Green Kit (Roche) according to the manufacturer's protocols. All the sample cDNAs and a calibration sample were amplified with specific oligonucleotide primers (see Tables 1, 2), previously validated for efficiency and specificity of amplification (denaturation profiles). Standard dilution curves were determined for every target cDNA. Samples were analysed in triplicate. To normalize for the amount of total RNA used in each reaction, we carried out amplification of mRNA for the house-keeping gene *GAPDH* (D-glyceraldehyde-3-phosphate dehydrogenase). Experiments were repeated twice on independent samples. Data analysis was performed with LightCycler software 3.5. (Roche).

Cell-cycle analysis

HC11 cells were plated in 6-well cluster dishes at a density of 7.5×10^4 cells/dish in GM and treated with AS *Tbx3* oligos as above. Cells were then trypsinized, fixed in ethanol 70% at 4°C and stored at 4°C. For analysis, $1–2\times10^6$ cells were washed, resuspended in PBS containing 10 μg/ml PI (Sigma) and 12.5 μl RNase and kept at 4°C for at least 12 h. The stained cells were then analysed on a Becton Dickinson FACS Calibur Flow cytometer equipped with a 488-nm laser. The PI red fluorescence pulse was detected at 620 nm and the distribution of the cells in the various cell-cycle phases was calculated by using CellFit software.

Results

Down-regulation of endogenous Tbx3 reduces growth rate of MECs

We applied the AS oligos designed to down-regulate *Tbx3* mRNA to MECs in culture. The depletion of *Tbx3* was confirmed by qPCR analysis of cDNA derived from AS-treated vs. untreated or S-treated cells. The reduction of *Tbx3* expression in AS-treated MECs was as follows: 41±5% and 21±3% for mouse HC11 and NulliB cells, respectively (Fig. 1a,b); 40±4% and 35±5% for rat LA7 and 106A10 cells, respectively (Fig. 1d,e); 49±5% and 52±6% for human MCF7 and MDA435 cells, respectively (Fig. 1c,f).

Cell proliferation was estimated by determining the number of metabolically active cells as a function of time in culture (MTT vital stain). Treatment of HC11 cells with the AS oligos resulted in a 38% reduction of their monolayer growth in GM, compared with S-oligo-treated and untreated cells (Fig. 1a). To verify that the inhibition of monolayer growth following AS treatment was not attributable to the toxicity of AS oligos and did not reflect activation of programmed cell death, we determined the apoptotic rate of AS-treated HC11 cells by staining with DAPI and directly counting apoptotic nuclei. We observed an extremely low fraction of apoptotic nuclei (less than 0.5%), with no significant differences in the AS-treated vs. untreated or control S-treated cells (data not shown).

Since HC11 cells harbour two mutated alleles of *p53*, and since the re-introduction of WT *p53* arrests their growth (Merlo et al. 1994, 1995), we reasoned that *p53* should be dispensable for *Tbx3* function. To examine this, we analysed the NulliB MEC line, derived from cultures of MECs of *p53*−/− mice (Medina and Kittrell 2003). The partial depletion of endogenous *Tbx3* in NulliB cells by AS treatment resulted in a 30±4% reduction in their monolayer growth (Fig. 1b). These data indicated the existence of a *p53*-independent *Tbx3*-mediated pathway of MEC growth.

We then evaluated the growth of MECs harbouring functional WT *p53*, upon partial depletion of *Tbx3*, by using the MCF7 human breast cancer cell line. The growth

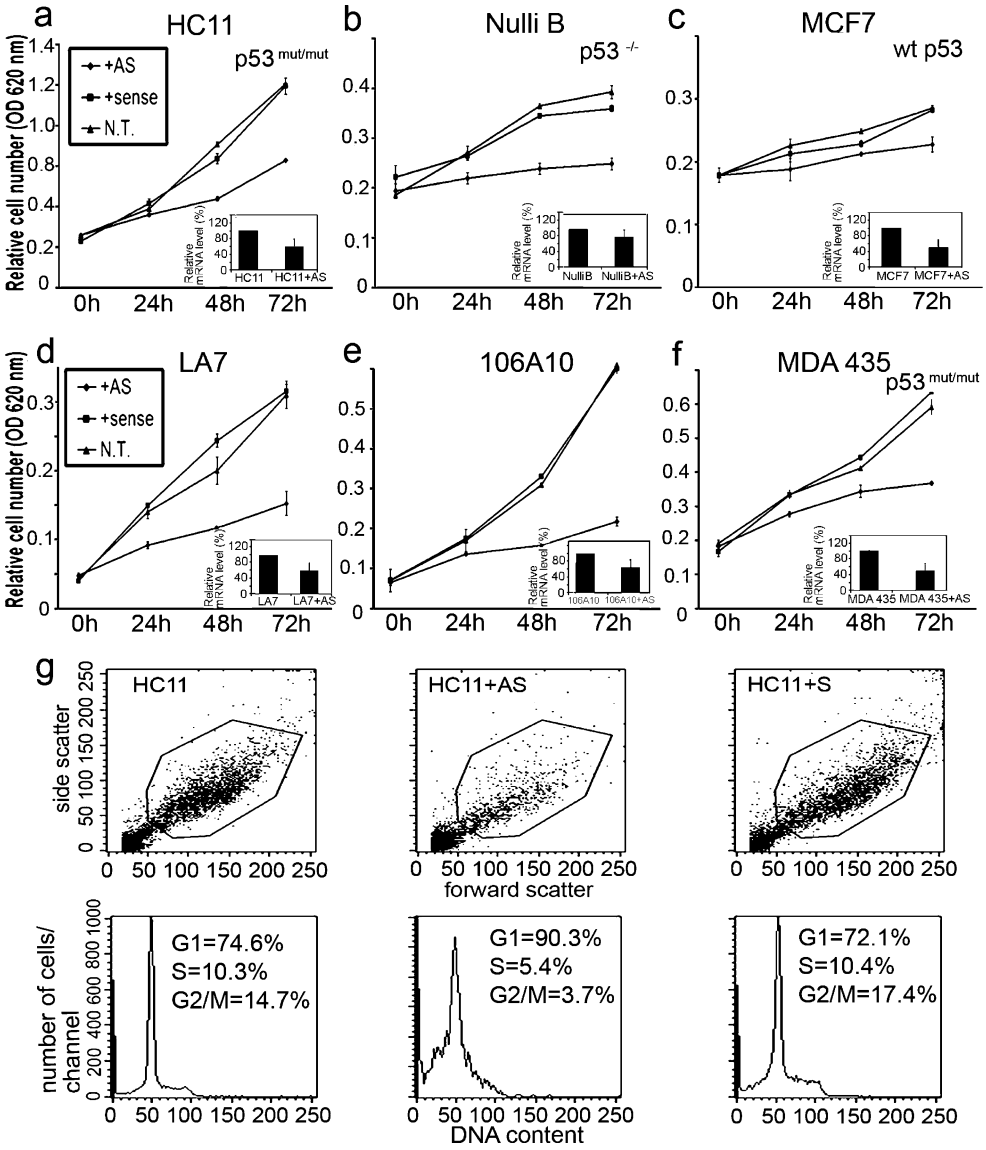

Fig. 1 Depletion of endogenous Tbx3 affects growth of MECs. **a–c** Growth curves of murine HC11 and NulliB MECs (**a, b**) and human MCF7 MECs (**c**) treated with antisense (AS) *Tbx3* oligos (+*AS*), control sense (S) oligos (+*sense*), or not treated (*N.T.*). **d, e** Growth of LA7 and 106A10 rat MECs treated with AS *Tbx3* and control S oligos. **f** Growth of MDA435 human breast carcinoma cells treated with AS *TBX3* or control S oligos. The *p53* status of the cell lines is indicated, if known. In each diagram, the level of *Tbx3* mRNA, determined by real-time qPCR in treated vs. N.T. cells is shown (*insets*, *bottom right*). The data are reported as the *Tbx3/GAPDH* ratio, the level of *Tbx3* in untreated cells being set at 100%. **g** DNA cell-cycle and forward/side scatter analysis of control untreated (*left*), AS-treated (*middle*) and S-treated (*right*) HC11 cells at 72 h after treatment (*top*). The calculated fraction of cells in G0/G1, S and G2/M phases are reported *bottom*

of these cells in the presence of AS *TBX3* oligos was reduced by 20±3% compared with S-oligo-treated and untreated cells (Fig. 1c). Thus, relative to cells with mutated or absent *p53*, AS treatment of MECs with WT *p53* gave a modest growth reduction. This may have been attributabale to the presence of non-functional (mutated) *p14ARF* in these cells (Kashuba et al. 2003), a transcriptional target of *Tbx3* (see below).

Next, we examined the growth properties of tumorigenic MECs upon partial depletion of *Tbx3* mRNA, by using the same AS procedure as before. In this set of experiments, we used LA7 and 106A10 rat MECs, two clones that were derived from the Rama-25 cell line (Dulbecco et al. 1979) and that recapitulate alveologenesis and tubulogenesis in vitro (Zucchi et al. 1998; Dulbecco et al. 1980; Dulbecco and Okada 1980). These cells are able to form structures that resemble ducts (early gland development), alveoli (lactogenic differentiation) or elongated myoepithelial cells and have been well characterized with regard to their proliferation, differentiation and apoptotic properties and their distinct pattern of gene expression (Dulbecco et al. 1980; Dulbecco and Okada 1980; Zucchi et al. 1998, 1999, 2002). In these cells, *Tbx3* depletion resulted in reduced cell growth (LA7 cells: −52±6%; 106A10 cells: −64±7%; Fig. 1d,e). Similarly, growth of *NeuT*-transformed HC11 cells was reduced by treatment with AS *Tbx3* oligos (data not shown). Finally, in the *TBX3*-expressing MDA435 mammary carcinoma cell line (with mutated *p53*), growth was reduced (−42±4%) upon *Tbx3* AS treatment (Fig. 1f). Thus, the data from both tumorigenic and non-tumorigenic MEC lines indicated that depletion of *Tbx3/TBX3* led to a reduction of cell growth in a *p53*-independent manner.

We subsequently carried out a cell-cycle assay on HC11 cells with depleted *Tbx3* expression by means of FACS

analysis. DNA histograms and dot plots of the forward vs. side-scatter of the control, AS-oligo-treated and S-oligo-treated cells, evaluated after 72 h, are presented in Fig. 1g. The results show that upon treatment with AS *Tbx3* oligos, the majority (90%) of the cells were in the G1 phase, with few in the S-early phases. These data indicated the Tbx3 regulated MEC growth by controlling(directly or indirectly) the G1/S checkpoint transition.

Differentiation and apoptosis are not affected by Tbx3 depletion

To examine the role of *Tbx3* in cell differentiation, we used the HC11 and LA7 MECs, which are able to differentiate in vitro under specific conditions. Confluent HC11 cells start to synthesize several milk proteins following induction with the lactogenic hormones dexamethasone, insulin and prolactin (DIP; Ball et al. 1988; Merlo et al. 1996). The ability of HC11 cells to differentiate was evaluated by detecting the expression of β-casein milk protein. First, we determined the relative abundance of *Tbx3* mRNA in differentiating HC11 cells compared with that of unstimulated cells by semi-quantative reverse transcription (RT)-PCR. Normalized to the level of *GAPDH* mRNA, levels of *Tbx3* mRNA in both cells were similar (Fig. 2a). Likewise, the human MCF10a MECs also showed no change in *TBX3* expression upon confluency and DIP treatment (data not shown). We then examined β-casein expression in HC11 cells induced to differentiate, comparing AS-oligo-treated vs. untreated cells. No significant difference was observed (Fig. 2b). Thus, depletion of *Tbx3* mRNA in HC11 cells did not affect either their competence to differentiate or their response to lactogenic hormones. Next, we examined LA7 cells; these cells spontaneously undergo differentiation by forming domes in confluent cultures, an effect that can be enhanced by addition of DMSO, lactogenic hormones, cAMP analogues, retinoic acid or lipids in the medium (Dulbecco et al. 1980; Dulbecco and Okada 1980; Zucchi et al. 2002). After reaching confluence, LA7 cells were exposed to 2% DMSO for 48 h. No significant difference in the number or size of domes was observed on comparing AS-treated LA7 cells vs. untreated cells (Fig. 2c). Thus, data from both cellular systems indicated that *Tbx3* depletion did not affect significantly MEC differentiation.

Finally, we determined whether the down-regulation of *Tbx3* mRNA had any effect on the survival of MECs. We applied conditions known to induce the apoptosis of MECs, reminiscent of the events taking place during the post-weaning involution of the MG (Merlo et al. 1996). We plated HC11 cells and maintained them in the confluent

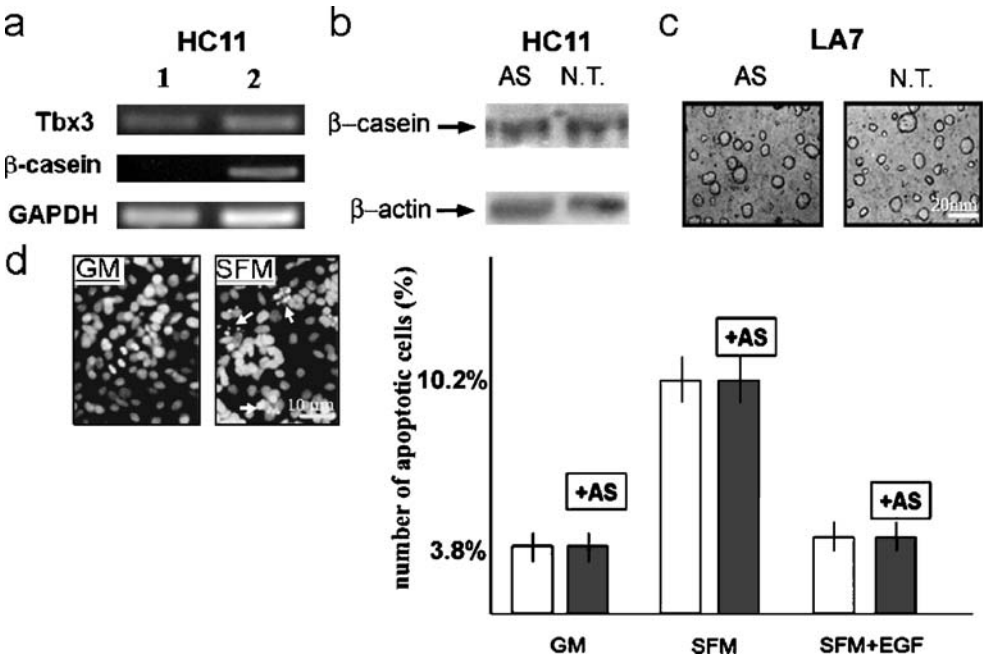

Fig. 2 Down-regulation of Tbx3 has no effect on differentiation and apoptosis MECs. **a** Semi-quantitative RT-PCR analysis to detect *Tbx3* mRNA in undifferentiated (*lane 1*) and differentiated (*lane 2*) HC11 cells. Amplification of β-casein mRNA is also shown to confirm differentiation. **b** Western blot detection of β-casein (with anti-milk protein antiserum) in HC11 cells, comparing AS-Tbx3-treated (*left*) and untreated (*right*) cells. β-Actin served as loading control (*N.T.* not treated). **c** Dome formation of LA7 cells following treatment with AS *Tbx3* oligos (*left*) or no treatment (*right*). LA7 cells were induced to differentiate with 2% DMSO. **d** *Right* Apoptosis of HC11 cells treated with AS *Tbx3* (+*AS*, *grey solid bars*) compared with untreated cells (*open bars*). Confluent cell cultures were maintained in growth medium (*GM*), serum-free medium (*SFM*) or serum-free medium plus epidermal growth factor (*SFM+EGF*). The results are expressed as the number of apoptotic nuclei over the total number of nuclei counted, in percent. The standard deviations of three independent experiments are shown. *Left* Micrographs showing apoptotic nuclei (*arrows*)

state, but deprived of serum, EGF and insulin, as described (Merlo et al. 1996). To estimate the number of apoptotic cells, we directly counted DAPI-stained nuclei with morphological features of apoptosis. We observed that AS-*Tbx3*-treated HC11 cells responded equally to confluence and serum/growth factor starvation, as compared with untreated cells (Fig. 2d). Furthermore, the addition of EGF to the starved cells restored cell survival in the presence or absence of AS *Tbx3*. Therefore, *Tbx3* seemed not to play an important role in MEC apoptosis and survival.

Effect of TBX3 overexpression on MECs growth, differentiation and apoptosis

Expression of the epitope-tagged HA-*TBX3* in the HC11 MECs was achieved by introducing an expression vector carrying the HA-*TBX3* cDNA under the control of the CMV promoter. Several clones (>30) were obtained and analysed for the expression and nuclear localization of HA-TBX3 by immunostaining with anti-HA antibody. Two clones were isolated that showed HA-TBX3 expression by Western and immunostaining analyses: clone 25 showed HA immuoreactivity in about 60±% of the nuclei, whereas clone 26 showed 30±5% of HA-positive nuclei (Fig. 3a,b). No puromycin-resistent clone could be obtained that stably expressed HA-*TBX3* in all nuclei, most likely because of the intolerance of these cells to the high expression of *TBX3*. Similarly, Carlson and coauthors (2002) reported that *Tbx3* expression appeared to be toxic to C2C12 myogenic cells.

The expression of exogenous *TBX3* mRNA in the transfected clones was quantified by qPCR analysis with primers specific to *hTBX3*. Clones 25 and 26 showed, respectively, a 6-fold and 4.8-fold increase in *TBX3* expression compared with endogenous *hTBX3* expression in the (human) MCF10a cells (Fig. 3a).

Clones 25 and 26 were monitored for their growth properties in monolayers. We expected to observe a promotion of monolayer growth in MECs expressing exogenous *TBX3*. Clone 25 cells (higher HA-*TBX3* expression) maintained in GM showed a 37±5% increase in their rate of monolayer growth, whereas clone 26 cells (lower expression) showed a 9±1% growth increase compared with HC11 cells transfected with empty plasmid (Fig. 3c). We examined the growth of these cells in reduced medium conditions (1% serum, no EGF): clone 25 and 26 cells showed, respectively, a 42±5% and a 30±4% increase in growth rate compared with control cells (Fig. 3d).

We then tested the ability of HA-*TBX3*-expressing HC11 cells to differentiate following the lactogenic stimulus. We carried out Western analysis to determine the β-casein protein level in total extracts of clone 25 and 26 cells treated with DIP mix. Upon induction, clone 25 and clone 26 cells were found to express β-casein to a level similar to that of the mock cells; however, clone 25 cells showed a slightly lower level (Fig. 3e). This reduced β-casein expression in clone 25 cells could have simply been a consequence of cell cloning. Nevertheless, these results suggested that the expression of exogenous *TBX3* did not greatly affect the capacity of MECs to respond to lactogenic hormones and initiate differentiation.

Next, we examined the apoptotic response of clone 25 and clone 26 cells to stress stimuli. We applied conditions known to induce apoptosis in these cells (Merlo et al. 1996) and estimated the rate of apoptosis by two independent assays: (1) DAPI nuclear staining and the direct counting of morphologically apoptotic nuclei and (2) flow cytometry for Annexin V-FITC. The number of early apoptotic cells in response to stress, as detected by flow cytometry, in clone 25 and clone 26 cells was not significantly different from that of the parental HC11 cells (Fig. 3f, top). Similarly, direct counting of apoptotic nuclei showed no significant difference in the fraction of morphologically apoptotic nuclei in clone 25 and 26 cells from that of the parental cells (Fig. 3f, bottom), suggesting that no differences occurred in the ability of these cells to activate their apoptotic program in response to the withdrawal of serum/growth factors.

TBX3-dependent regulation of ARF expression and other members of cell-cycle regulation in MECs

In EF and other non-epithelial cells, *TBX3* can repress the expression of the cell-cycle regulatory gene *ARF*, resulting in their immortalization in the presence of WT *p53* (Carlson et al. 2001; Brummelkamp et al. 2002). Both the repression domain and the T-box (DNA-binding) domains of TBX3 are required to mediate *ARF* repression in EFs. Here, we have investigated the ability *TBX3* to repress transcription of *p14ARF* (*p19ARF* in murine cells) in MECs lacking functional *p53*.

Luciferase reporter assays were carried out by using a *p14ARF* promoter fragment previously shown to mediate a strong dose-dependent repression in EFs, via an element located in the region of −19 to +54 of *p14ARF* (Jacobs et al. 2000; Lingbeek et al. 2002; Brummelkamp et al. 2002). Various MEC lines were transiently co-transfected with the *ARF* promoter-reporter plasmid and with 5 μg of the HA-*TBX3* expression plasmid, followed by measurement of the relative luciferase activity in the cells. In cells lacking WT *p53*, we observed a significant repression of the *ARF* promoter activity by TBX3 (−77±6% and −64±5% for, respectively, HC11 and NulliB cells; Fig. 4a). As a control, in non-MECs, viz. COS-7 cells (harbouring inactive p53), we observed a 50±5% inhibition of *ARF* promoter activity. The tumorigenic MEC lines LA7 (unknown p53 status) and

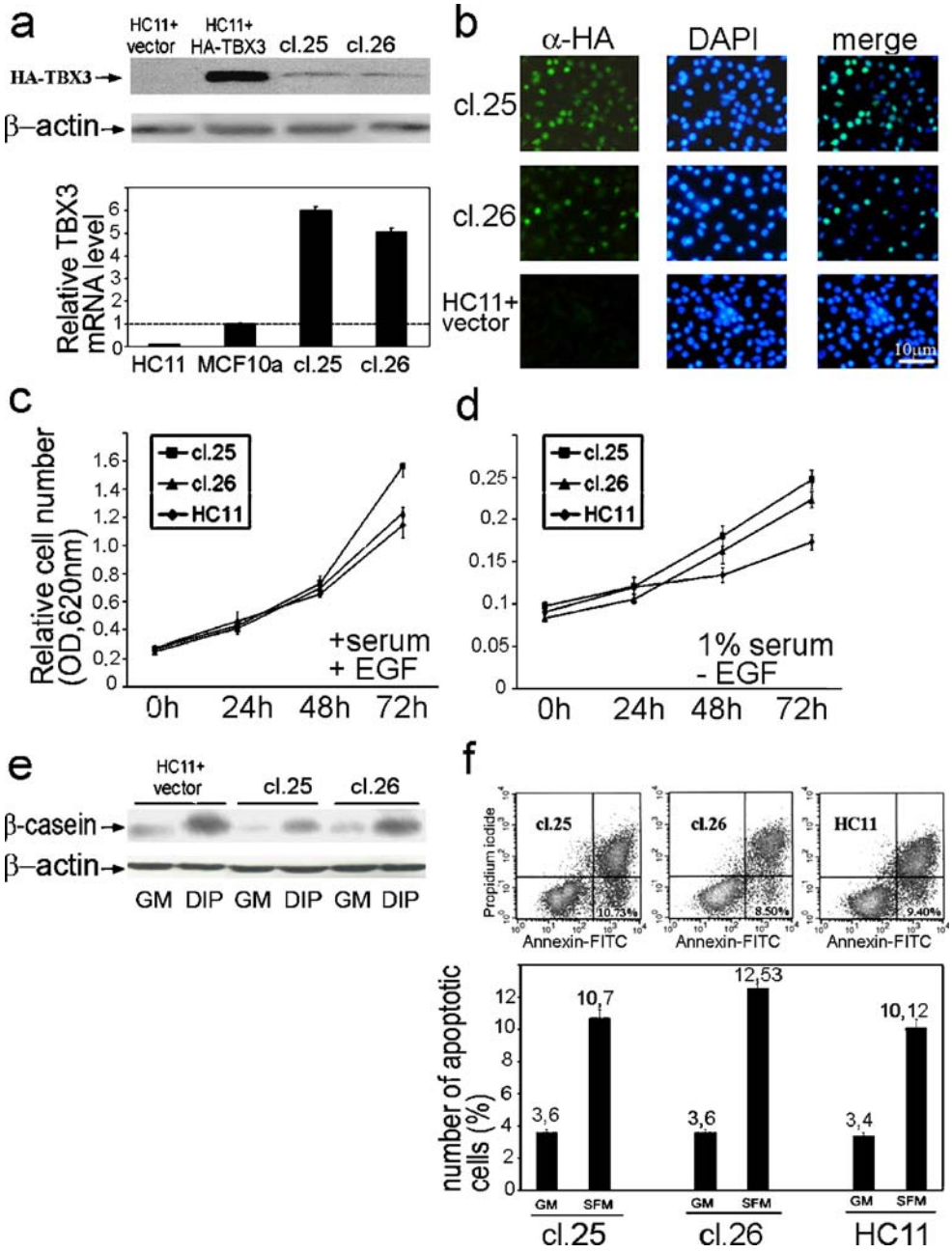

Fig. 3 Overexpression of HA-TBX3 promotes growth of MECs. **a** *Top* Western blot analysis to detect HA-TBX3 fusion protein in two clones (*cl.25*, *cl.26*) transfected with the *HA-TBX3* plasmid. Expression of HA-*TBX3* in transiently transfected HC11 cells and in cells transfected with the empty vector are also shown, for comparison. *Bottom* Relative abundance of exogenous HA-*TBX3* mRNA compared with endogenous *TBX3* expression in the (human) MCF10a cells, as determined by real-time qPCR. The data are represented as the ratio *TBX3/GAPDH*, the expression in MCF10a cells being set to 1. In untransfected HC11 cells, the expression of (human) *TBX3* was negligible. **b** Immunostaining of clone 25 (*cl.25*) and clone 26 (*cl.26*) cells compared with vector-transfected HC11 cells (*bottom*) to detect HA-TBX3. Nuclei are visualized with DAPI. HA immunoreactivity is localized in the nuclei. **c**, **d** Growth of HA-*TBX3*-expressing clone 25 and 26 cells (*cl.25*, *cl.26*) compared with HC11 cells transfected with vector only (*HC11*), in GM (**c**) or in reduced medium (**d**). **e** Differentiation of clone 25 and 26 cells (*cl.25*, *cl.26*) compared with HC11 cells transfected with vector only (*HC11+vector*). Confluent cultures were incubated in DIP medium or in GM and then analysed for β-casein expression by Western blot. β-Actin (*bottom*) was used as control for sample loading. **f** Apoptosis of clone 25 and 26 cells (*cl.25*, *cl.26*) compared with parental HC11 cells (*HC11*). *Top* Flow cytometry relative to clone 25 (*left*), clone 26 (*middle*) and control HC11 cells (*right*), reporting propidium iodide (*y axis*) vs. Annexin-V FITC (*x-axis*). The *dots* represent individual events from a population of 10,000 events analysed. The calculated percentages of early apoptotic cells are reported for each cell population (*bottom right*). *Bottom* Direct counting of apoptotic nuclei in the same cell populations as above. The results are expressed as the percentage of apoptotic nuclei over the total number of nuclei counted. All experiments were performed three times; the standard deviations are shown

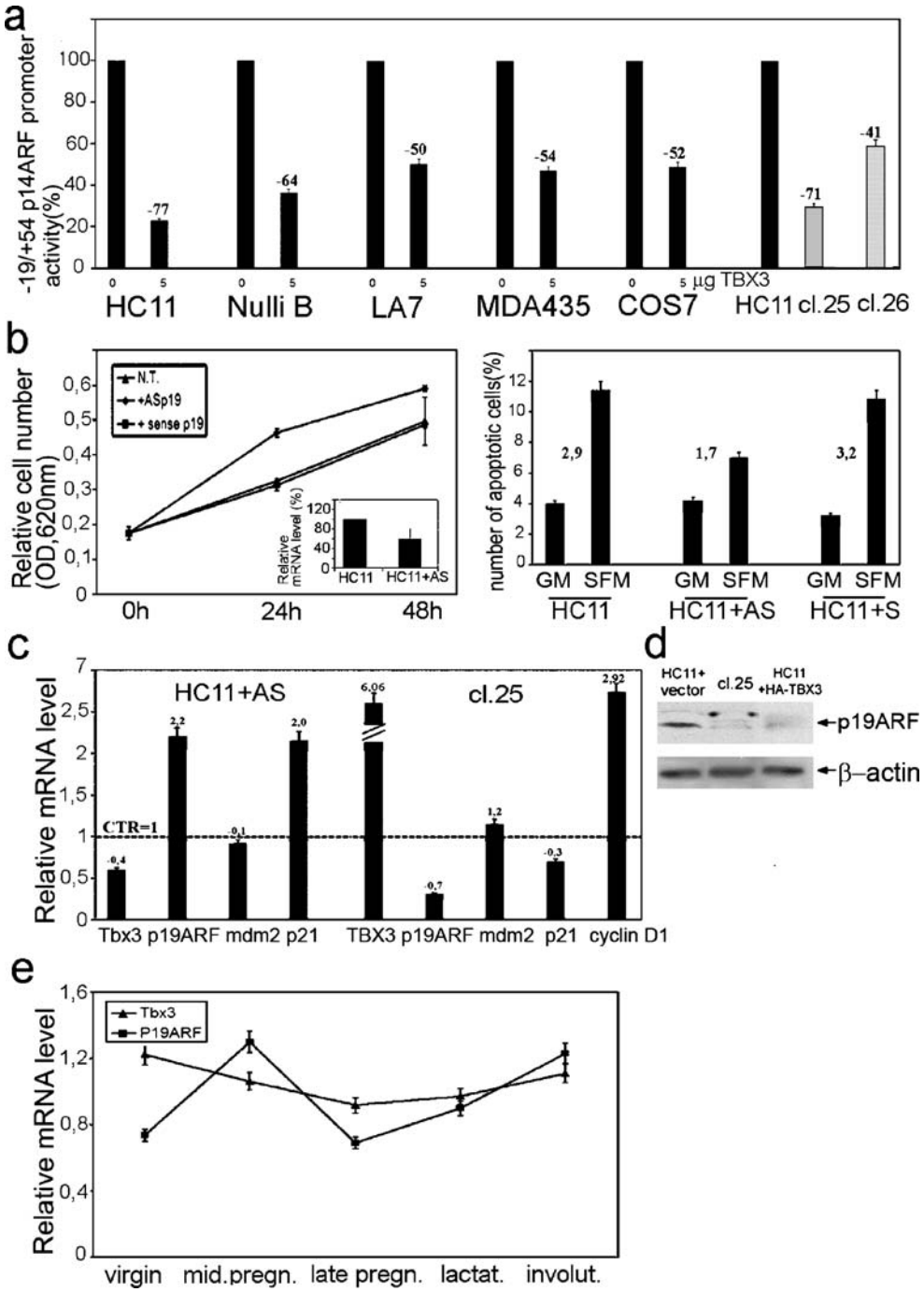

MDA-435 cells (mutant *p53*; Docquier et al. 2005) showed an inhibition of approximately 50% of the *ARF* promoter activity by TBX3. On analysing the *ARF* promoter activity in clone 25 and 26 cells expressing HA-*TBX3*, we observed reduced *ARF* promoter transcription (−71±2% and −41± 2% in clone 25 and clone 26 cells, respectively) compared with HC11 parental cells (Fig. 4a). The degree of *ARF* promoter inhibition was correlated with the *TBX3* expression level: clone 25 with higher *TBX3* expression showed stronger inhibition and vice versa. These data together indicated that *TBX3* suppressed *ARF* transcriptional activity via the −19 to +54 promoter element in MECs. This regulation took place in the absence of WT *p53* and therefore was independent of the p53 cell-cycle regulatory pathway.

Subsequently, we investigated whether the depletion of *p19ARF* mRNA could lead to the enhanced growth of MECs. We applied an AS oligo strategy to HC11 by designing two synthetic 21-nucleotide AS oligos specifically to target *p19ARF* and not *p16INK4A*. A 40±3% reduction in *p19ARF* mRNA was observed in HC11 following AS-*p19ARF*-oligo treatment, in comparison with

◀ **Fig. 4** TBX3 negatively regulates the ARF promoter, irrespective of p53 and Mdm2. **a** *Left* Repression of the (−19/+54) *ARF* promoter by *TBX3* (*5*) in MEC lines and COS-7 cells by luciferase-reporter assay (*black bars*). The basal promoter activity (transfection with empty vector) is set at 100% in each case (*0*). *Right* Level of the (−19/+54) *p14ARF* promoter activity in clone 25 and 26 cells (*light grey bars*). Experiments were performed at least three times; the standard deviations are indicated. **b** *Left* Growth curves of HC11 treated with AS *p19ARF* (+*ASp19*) and control S oligos (+*sense p19*) compared with that of parental HC11 (*N.T.*). The level of *p19ARF* mRNA determined by real-time qPCR in treated vs. N.T. cells is shown in the insets (*bottom right*). The data are reported as the *p19ARF/GAPDH* ratio, the level of *p19ARF* in untreated cells being set at 100%. *Right* Apoptosis assay of HC11 cells treated with AS *p19ARF* (+*AS*) compared with cells treated with S oligos (+*S*) and with parental HC11 cells. The experimental conditions were the same as in Fig. 1k. Fold change is shown, compared between the effect on apoptotic rate in SFM and GM. The standard deviations between independent experiments are shown. **c** Endogenous levels of *Tbx3*, *p19ARF*, *Mdm2*, $p21^{CIP1/WAF}$ and *cyclin D1* mRNAs determined by real-time qPCR in HC11 cells treated with AS *Tbx3* and in clone 25 cells expressing exogenous HA-*TBX3*. Values were normalized to *GAPDH* mRNA. The level of mRNAs in parental HC11 cells was set at 1 (*horizontal dashed line*). For quantification of TBX3 expression in clone 25 cells, the endogenous level of TBX3 in human MCF10a cells served as a control and was set at 1. The standard deviations between independent experiments are shown. **d** Western blot detection of p19ARF in clone 25 (*cl.25*) cells (*middle lane*), in HC11 transiently transfected with *HA-TBX3* (*right lane*) and in HC11 cells transfected with empty expression vector (*left lane*). The β-actin level served as a loading control. **e** In vivo expression of *Tbx3* and *p19ARF* during postnatal maturation of the mammary gland. Gland nos. 4–5 from WT adult females, at the indicated stages (*mid.* middle, *pregn.* pregnancy, *lactat.* lactation, *involut.* involution) were dissected, pooled, extracted for RNA and analysed by real-time qPCR (see Materials and methods). The relative abundance of *Tbx3* and *p19ARF*, normalized to *GAPDH* mRNA, is shown. A calibration sample was used (a mixed pool of cDNAs from all stages); the mRNA abundance was set at 1

untreated cells, by qPCR (Fig. 4b). After 24 and 48 h of AS treatment, HC11 cells showed, respectively, a 40±4% and a 20±2% enhancement of monolayer growth compared with untreated cells or S-oligo-treated cells (Fig. 4b). Longer treatment resulted in cell toxicity.

Next, we determined the rate of apoptotic death in HC11 cells upon depletion of *p19ARF* mRNA. p19ARF has been shown to play a role in the balance between cell proliferation and apoptosis during, respectively, pregnancy and involution of the MG (Yi et al. 2004). We applied the same conditions (as above; known to induce apoptosis) to AS- and S-treated cells and observed a reduced induction of apoptotic death (1.7-fold) upon depletion of *p19ARF* compared with S-treated or parental cells (2.9-fold and 3.2-fold, respectively, Fig. 4b, right). These results indicated that reduced *p19ARF* levels could slightly affect monolayer cell growth independently of p53 and modified the apoptotic response of MECs to stress stimuli.

We then determined whether altered *Tbx3* expression could affect expression of other components of cell-cycle regulation in HC11 cells. ARF is known to associate with Mdm2, causing its re-localization to nucleoli and preventing ubiquitination and nuclear export of p53 (Sherr 1998; Weber et al. 1999). Active p53, in turn, promotes the transcription of target genes, such as the CDK inhibitor $p21^{CIP1/WAF}$ (Brugarolas et al. 1995), and induces growth arrest, senescence or apoptosis. We speculated that Tbx3 might suppress transcription of $p21^{CIP1/WAF}$, since Tbx2, a T-box protein homologous to Tbx3, can repress $p21^{CIP1/WAF}$ expression (Prince et al. 2004). We therefore determined the level of endogenous expression of *p19ARF*, *Mdm2* and $p21^{CIP1/WAF}$ in HC11 cells in which endogenous *Tbx3* had been partially depleted. qPCR analysis showed a 2.2-fold increase of *p19ARF* expression in HC11 treated with AS *Tbx3* oligos, compared with control cells (Fig. 4c). However, expression of *Mdm2* was not changed in the AS-*Tbx3*-treated cells (Fig. 4c). Upon depletion of *Tbx3*, the expression of $p21^{CIP1/WAF}$ in HC11 cells was elevated two-fold, compared with control cells (Fig. 4c). Next, we determined p*19ARF*, *Mdm2*, $p21^{CIP1/WAF}$ and *cyclin D1* mRNA abundance in cells over-expressing HA-*TBX3*, by qPCR. In clone 25 cells expressing a higher level of HA-*TBX3* (6-fold more than endogenous; Fig. 4c), we detected a decrease (−70±3%) in the *p19ARF* mRNA level. A reduced p19ARF protein level was consistently detected in clone 25 cells by Western blot analysis (Fig. 4d). Decreased expression of $p21^{CIP1/WAF}$ (−30±2%) was observed in clone 25 cells (Fig. 4c), whereas no significant changes in *Mdm2* expression were detected. Finally, we determined the expression of *cyclin D1* in cells over-expressing HA-*TBX3*. Cyclin D1 is one of the main regulators of the G1/S-phase transition (Resnitzky and Reed 1995) and is over-expressed in a high fraction of breast tumor cell lines and primary tumors (Weinstat-Saslow et al. 1995). We observed a three-fold increased level of *cyclin D1* mRNA in clone 25 cells compared with that of parental cells, consistent with reported data on the repression of cyclin D1 by p19ARF utilizing both the p53-dependent and -independent pathways (D'Amico et al. 2004). Similar results were obtained with clone 26 with less drastic changes (data not shown). Taken together, these data indicated that TBX3 could regulate *p19ARF,* $p21^{CIP1/WAF}$ and *cyclin D1* expression in MECs lacking functional WT *p53*, irrespective of the Mdm2-p53-dependent pathway.

Finally, we examined the expression of *Tbx3* and *p19ARF* within the context of a tissue subjected to physiological stimuli. We extracted RNA from MGs at various postnatal stages, including virgin (10 weeks), mid-pregnancy (10 days), late pregnancy (15 days), lactation (2–4 days) and involution (2 days) stages. We then compared the relative abundance of *Tbx3* and *p19ARF* mRNA by qPCR. The *Tbx3* mRNA level was slightly higher in virgin MGs but then declined during pregnancy and remained nearly unchanged in all subsequent steps

(Fig. 4e). The *p19ARF* mRNA level was nearly undetectable in virgin glands, increased at mid-pregnancy and declined at late pregnancy. During lactation (2–4 days) and involution (2 days), an increase was observed in the relative *p19ARF* mRNA level (Fig. 4e). These data indicated that *Tbx3* expression in normal MGs remained unchanged during its maturation stages and was sufficient to provide the MECs with the growth properties characteristic of that stage. Hence, *Tbx3* expression is unlikely to be hormonally controlled, whereas *p19ARF* expression is known to respond to hormonal changes during pregnancy, as is consistent with our results.

Discussion

Haploinsufficiency of the *TBX3* gene product is the recognized cause of UMS. The breast defects in UMS patients vary from mild hypoplasia to the absence of the areola and the inability to lactate (Bamshad et al. 1997, 1999; Meneghini et al. 2006). In mice with homozygous inactivation of *Tbx3*, the MGs fail to develop altogether, whereas mild defects in MG development are observed in heterozygous adult females (Davenport et al. 2003; Jerome-Majewska et al. 2005). Since *TBX3* is expressed in the MECs of the ductal and lobule-alveolar system (Davenport et al. 2003; Chapman et al. 1996), a cell-autonomous role of this transcription factor in regulating the growth of MECs seems obvious, although a direct demonstration is lacking. Here, we have addressed the cellular functions of *TBX3* by using several MEC lines in vitro. We show that *TBX3* inhibits the transcription of *ARF* and promotes cell growth independently of the *p53* pathway of cell-cycle regulation. These observations suggest that the *Tbx3* expression level is critical for confering growth ability on MECs. Since the cellular targets of *TBX3* mutations in vivo are the limb buds and the apocrine glands, and in particular the MG, we considered it rational to establish *Tbx3* function in MECs. By altering *Tbx3* expression, we show for the first time an involvement of *Tbx3* in the regulation of MEC growth.

MECs appear to use a pathway distinct from that known in EFs or other non-epithelial cells (Carlson et al. 2001; Brummelkamp et al. 2002; Lingbeek et al. 2002), as *TBX3* controls the growth rate independently of *p53*. To establish this, we have used MEC lines that harbour WT (MCF7) or mutated *p53* (HC11, MDA435) or that are devoid of *p53* (NulliB). All these cell lines are sensitive to the AS-mediated down-regulation of *Tbx3* expression. Similarly, the growth of osteoblasts and bladder cells with mutated *p53* is inhibited upon depletion of *Tbx3* (Govoni et al. 2006; Ito et al. 2005). To reinforce the point that *TBX3* acts in a p53-independent way, the absence of *p53* cannot rescue the mild MG phenotype observed in *Tbx3*+/− mice (Jerome-Majewska et al. 2005). As we have excluded p53, *Tbx3*-mediated MECs growth is likely to entail the repression or activation of other growth regulatory proteins. We have examined the expression of the cell-cycle negative regulator *p19ARF*. This gene is regulated by Tbx2 and Tbx3 in non-epithelial cells, acts upstream of *p53* and can lead to cell immortalization when abnormally expressed (Carlson et al. 2001; Brummelkamp et al. 2002; Lingbeek et al. 2002; Carnero et al. 2000). Here, we show that Tbx3 represses *ARF* transcription in MECs via the (−19/+54) promoter element; the data have been confirmed by the up-regulation of endogenous *p19ARF* mRNA in cells with a reduced level of *Tbx3* mRNA. Consistent with the finding that p19ARF represses the expression of *cyclin D1* (D'Amico et al. 2004), we have detected increased *cyclin D1* expression in HC11 cells over-expressing *TBX3*. Finally, we have demonstrated that the depletion of endogenous *p19ARF* in MECs results in a slight promotion of cell growth. Moreover, in MCF7 cells, which contain WT *p53* but mutated *p14ARF* (Kashuba et al. 2003), the depletion of endogenous *TBX3* results in a modest inhibition of growth compared with that of other MECs. Collectively, these results indicate that *Tbx3* utilizes a p19ARF-dependent p53-independent pathway to control MEC growth.

ARF is commonly accepted to induce p53-dependent growth arrest by sequestering the p53 antagonist Mdm2 protein in the nucleolus (Sherr 1998; Weber et al. 1999). In EFs with WT p53, the down-regulation of *ARF* leads to an extended lifespan and cell immortalization (Carnero et al. 2000). On the contrary, our data on MECs indicate that WT *p53* is not required for Tbx3-ARF-mediated growth regulation. Alternatively, *p53*-independent ARF functions have been recognized: the reintroduction of p19*ARF* in EFs lacking *p53*, *Mdm2* and *p19ARF* arrests their proliferation (Weber et al. 2000). Several other mechanisms and targets have also been proposed (Datta et al. 2002; Normand et al. 2005; Sugimoto et al. 2003; Yarbrough et al. 2002) highlighting the complexity of p19ARF functions and suggesting the existence of distinct cell-type-specific pathways. By using appropriate cell models, such as MECs as opposed to EFs, some hypotheses regarding cell-cycle regulation may therefore need to be re-assesses.

We have evaluated the expression of Mdm2 and $p21^{CIP1/WAF}$; two cell-cycle control proteins that utilize both p53-dependent and -independent pathways. ARF is thought to neutralize the activity of Mdm2, an oncoprotein involved in a negative feedback loop with p53 (Momand and Zambetti 1997). Mdm2 has also been shown to be an effector of p19ARF in the absence of WT p53 (Steinman et al. 2004). We have found no significant change in *Mdm2* expression upon alteration of *Tbx3* expression, thus excluding its Tbx3-dependency and indicating an Mdm2-independent

ARF function (Korgaonkar et al. 2002). $p21^{CIP1/WAF}$ is a cyclin-CDK inhibitor that mediates p53-dependent growth arrest and that has been implicated in cellular senescence (Brown et al. 1997; Gartel and Tyner 2002). $p21^{CIP1/WAF}$ can also be activated by p53-independent stimuli leading to growth arrest, apoptosis or cell differentiation (Wang et al. 1999). We have observed changes in $p21^{CIP1/WAF}$ levels following altered *Tbx3* expression, consistent with an inhibitory function of Tbx3 on $p21^{CIP1/WAF}$ and with the increase of the growth rate of these cells. Interestingly, in melanoma cells, $p21^{CIP1/WAF}$ is repressed by Tbx2, a gene highly homologous to Tbx3 (Prince et al. 2004). Further analyses are needed to clarify whether the *Tbx3*-mediated regulation of $p21^{CIP1/WAF}$ in MECs is direct and to identify additional *Tbx3* downstream targets.

We have examined the effect of *Tbx3* over-expression or depletion on cell differentiation and apoptosis. HC11 and LA7 cells have provided us with two independent models of in vitro differentiation (Merlo et al. 1995; Zucchi et al. 1998), although alterations in *Tbx3* levels do not result in significant changes. We have also applied conditions known to induce apoptosis in HC11 cells, reminiscent of the events that take place during post-weaning involution of the MG (Merlo et al. 1996). Alterations of the *Tbx3* mRNA level have no significant effect on the ability of HC11 cells to activate their apoptotic program. The same results have been obtained with other MEC lines (N. Platonova, unpublished data). Finally, the endogenous expression of *Tbx3* in differentiating HC11 cells and in murine MGs during various physiological phases (virgin, pregnancy, lactation and involution) does not change. Thus, the only function of *TBX3/Tbx3* in MECs appears to be the control of growth properties.

During MG development, the first phase of epithelial cell proliferation is hormone-independent and generates the primitive ductal tree, the alveolar structure and the end buds. A second and a third phase occur, respectively, at puberty and during pregnancy and are hormone-dependent. The role of *Tbx3*, *p19ARF* and $p21^{CIP1/WAF1}$ in the expansion of the MEC population and in their differentiation and apoptosis in vivo is far from being understood. In *p19ARF*−/− mice, MGs grow and differentiate normally, with no obvious defects (Jerome-Majewska et al. 2005; Yi et al. 2004). However, in the absence of *p19ARF*, a larger number of MECs are in S-phase during pregnancy, whereas MECs from *ARF*−/− MGs readily give rise to immortalized clones in vitro, as do the *p53*−/− MECs (Yi et al. 2004; Jerry et al. 1998). Thus, *p19ARF* negatively contributes to the maintenance of a normal proliferation rate. On the contrary, *p19ARF* expression is low or undetectable in quiescent MECs, increases during mid-pregnant proliferation and is stimulated by hormone treatment (Sherr 1998; Yi et al. 2004). Therefore, the possible cell-cycle inhibitory function of *p19ARF* during pregnancy-dependent MEC proliferation is not consistent with its expression profile. The proliferation of MECs within the MG tissues is likely to entail higher-order regulation that depends upon tissue interactions and hormonal stimulation.

The up-regulation of *p19ARF* during pregnancy might reflect expression in non-epithelial cells (i.e. stromal cells). Indeed, *Tbx2* is mainly expressed in the stromal compartment of the MG (Chapman et al. 1996) and Tbx2 can repress *ARF* transcription in vitro (Paxton et al. 2002; Jacobs et al. 2000). Coincidently with the rise in *p19ARF* expression, *Tbx2* is down-regulated at mid-pregnancy (N. Platonova, unpublished data), further supporting the possibility that transcription regulation of *ARF* involves similar, but not identical, molecules in different cell types.

A more evident function of *p19ARF* in the adult MG is related to the activation of apoptosis during the post-weaning involution phase. In *ARF*−/− adult females, a reduced number of MECs undergoes apoptosis (Yi et al. 2004) and *p19ARF* expression is elevated during late involution, as compared with resting glands (Yi et al. 2004). This phenotype is shared with *p53*−/− mice, which also show delayed MG involution (Jerry et al. 1998). *Tbx3* is unlikely to play a role in this process, as we have seen no significant changes in *Tbx3* expression in normal MGs during involution and no changes in the apoptotic response of MECs to stress conditions when *Tbx3* expression is altered.

The partial down-regulation of *Tbx3* mRNA results in reduced MECs growth. Several human disorders linked to *T-box* gene mutations reveal a mechanism of haploinsufficiency (Packham and Brook 2003). Such is the case for *TBX5* in Holt-Horam syndrome (OMIM 142900; Basson et al. 1997; Li et al. 1997) and for *TBX1* in the DiGeorge-related syndromes (OMIM 188400, 192430, 217095; Jerome and Papaioannou 2001; Lindsay et al. 2001; Merscher et al. 2001). In X-linked cleft palate/ankyloglossia (OMIM 303400), a fraction of women with mutated *TBX22* exhibit the phenotype, suggesting haploinsufficiency with low penetrance (Braybrook et al. 2001; Marcano et al. 2004). The underlying notion is that the cellular level of the *T-box* gene products must be finely regulated to ensure proper cell growth, morphogenesis and differentiation.

Haploinsufficiency has been thought to be a feature of human pathologies, since mice heterozygous for the inactivation of *Tbx1*, *Tbx3* and *Tbx4* exhibit minimal or no evident defects (Jerome and Papaioannou 2001; Lindsay et al. 2001; Merscher et al. 2001; Davenport et al. 2003; Naiche and Papaioannou 2003). However, $Tbx5^{del/+}$ mice show all the phenotypes of Holt-Horam patients (Bruneau et al. 2001; Moskowitz et al. 2004), and the MGs of *Tbx3*+/−

adult mice develop normally but show reduced ductal branching (Jerome-Majewska et al. 2005). This indicates that half of the normal dose of *Tbx3* is not sufficient to complete postnatal morphogenesis of the gland epithelium. In these mice, however, the effect of *Tbx3* hemizygosity on pregnancy, lactation and involution and on the expression of *p19ARF* have not been examined and could be highly informative.

Acknowledgements We are grateful to Dr. M. Lingbeek (The Netherlands Cancer Institute, Amsterdam) and Drs. P. Hurlin and S. Ota (Shriners Hospitals, Portland, USA) for the generous gift of plasmids and to Dr. N. Hynes (Friedrich Miescher Institute, Basel, Switzerland) and Dr. D. Medina (Baylor College of Medicine, Houston, USA) for the HC11 and NulliB cells. We thank Dr. S. Mantero (Dulbecco Telethon Institute, Milano), Dr. E. Erba (Mario Negri Institute, Milano) and Dr. S. Carrabino (Cystic Fibrosis Institute, Milano) for technical assistance.

References

Ball R, Friis R, Schoenenberger C, Doppler W, Groner B (1988) Prolactin regulation of b-casein expression and of a cytosolic 120 kDa protein in a cloned mouse mammary epithelial cell. EMBO J 7:2089–2095

Bamshad M, Lin R, Law D, Scott Watkins W, Krakowiak P, Moore M, Franceschini P, Lala R, Holmes L, Gebuhr T, Bruneau B, Schinzel A, Seidman J, Seidman C, Jorde L (1997) Mutations in human TBX3 alter limb, apocrine and genital development in ulnar-mammary syndrome. Nat Genet 16:311–315

Bamshad M, Le T, Watkins W, Dixon M, Kramer B, Roeder AD (1999) The spectrum of mutations in Tbx3. Am J Hum Genet 64:1550–1562

Basson C, Bachinsky D, Lin R, Levi T, Elkins M (1997) Mutations in human TBX5 cause limb and cardiac malformation in Holt-Oram syndrome. Nat Genet 15:30–35

Braybrook C, Doudney K, Marcano A, Arnason A, Bjornsson A, Patton M, Goodfellow P, Moore G, Stainer P (2001) The T-box transcription factor gene TBX22 is mutated in X-linked cleft palate and ankyloglossia. Nat Genet 29:179–183

Brown JP, Wei W, Sedivy JM (1997) Bypass of senescence after disruption of p21CIP1/WAF1 gene in normal diploid human fibroblasts.Science 277:831–834

Brugarolas J, Chandrasekaran C, Gordon JI, Beach D, Jacks T, Hannon GJ (1995) Radiation-induced cell cycle arrest compromised by p21 deficiency. Nature 377:552–557

Brummelkamp T, Kortlever R, Lingbeek M, Trettel F, MacDonald M, Lohuizen M van, Bernards R (2002) TBX3, the gene mutated in ulnar-mammary syndrome, is a negative regulator of p19ARF. J Biol Chem 277:6567–6572

Bruneau BG, Nemer G, Schmitt JP, Charron F, Robitaille L, Caron S, Conner DA, Gessler M, Nemer M, Seidman CE, and Seidman JG (2001) A murine model of Holt-Oram syndrome defines roles of the T-box transcription factor Tbx5 in cardiogenesis and disease. Cell 106:709–721

Butz NV, Campbell CE, Gronostajski RM (2004) Differential target gene activation by TBX2 and TBX2VP16: evidence for activation domain-dependent modulation of gene target specificity. Gene 342:67–76

Carlson H, Ota S, Campbell C, Hurlin P (2001) A dominant repression domain in TBX3 mediates transcription repression and cell immortalization: relevance to mutations in TBX3 that cause ulnar-mammary syndrome. Hum Mol Genet 10:2403–2413

Carlson H, Ota S, Song Y, Chen Y, Hurlin P (2002) Tbx3 impinges on the p53 pathway to suppress apoptosis, facilitate cell transformation and block myogenic differentiation. Oncogene 21:3827–3835

Carnero A, Hudson JD, Price CM, Beach DH (2000) p16INK4A and p19ARF act in overlapping pathways in cellular immortalization. Nat Cell Biol 2:148–155

Carreira S, Dexter TJ, Yavuzer U, Easty DJ, Goding CR (1998) Brachyury-related transcription factor Tbx2 and repression of the melanocyte-specific TRP-1 promoter. Mol Cell Biol 18:5099–5108

Chapman D, Garvey N, Hancock S, Alexiou A, Agulnik S (1996) Expression of the T-box family genes, TBX1-TBX5 during early mouse development. Dev Dyn 206:379–390

Coletta RD, Jedlicka P, Gutierrez-Hartmann A, Ford HL (2004) Transcriptional control of the cell cycle in mammary gland development and tumorigenesis. J Mammary Gland Biol Neoplasia 9:39–53

D'Amico M, Wu K, Fu M, Rao M, Albanese C, Russell RG, Lian H, Bregman D, White MA, Pestell RG (2004) The inhibitor of cyclin-dependent kinase 4a/alternative reading frame (INK4a/ARF) locus encoded proteins p16INK4a and p19ARF repress cyclin D1 transcription through distinct cis elements.Cancer Res 64:4122–4130

Daniel CW, Smith GH (1999) The mammary gland: a model for development. J Mammary Gland Biol Neoplasia 4:3–8

Danielson K, Osborn C, Durban E, Butel J, Medina D (1984) Epithelial mouse mammary cell line exhibiting normal morphogenesis in vivo and functional differentiation in vitro. Proc Natl Acad Sci USA 81:3756–3760

Datta A, Nag A, Raychaudhuri P (2002) Differential regulation of E2F1, DP1, and the E2F1/DP1 complex by ARF. Mol Cell Biol 22:8398–8408

Davenport T, Jerome-Majewska L, Papaioannou V (2003) Mammary gland, limb and yolk sac defects in mice lacking TBX3, the gene mutated in human ulnar mammary syndrome. Development 130:2263–2273

Docquier F, Farrar D, D'Arcy V, Chernukhin I, Robinson AF, Loukinov D, Vatolin S, Pack S, Mackay A, Harris RA, Dorricott H, O'Hare MJ, Lobanenkov V, Klenova E (2005) Heightened expression of CTCF in breast cancer cells is associated with resistance to apoptosis. Cancer Res 15:5112–5122

Dulbecco R, Okada S (1980) Differentiation and morphogenesis of mammary cells in vitro. Proc R Soc Lond [Biol] 208:399–408

Dulbecco R, Bologna M, Unger M (1979) Differentiation of a rat mammary cell line in vitro. Proc Natl Acad Sci USA 76:1256–1260

Dulbecco R, Bologna M, Unger M (1980) Control of differentiation of a mammary cell line by lipids. Proc Natl Acad Sci USA 77:1551–1555

Gartel AL, Tyner AL (2002) The role of the cyclin-dependent kinase inhibitor p21 in apoptosis. Mol Cancer Ther 1:639–649

Govoni KE, Lee SK, Chadwick RB, Yu H, Kasukawa Y, Baylink DJ, Mohan S (2006) Whole genome microarray analysis of growth hormone induced gene expression in bone: T-box3, a novel transcription factor, regulates osteoblast proliferation. Am J Physiol Endocrinol Metab 291:E128–E136

Groner B (2002) Transcription factor regulation in mammary epithelial cells. Domest Anim Endocrinol 23:25–32

He ML, Wen L, Campbell CE, Wu JY, Rao Y (1999) Transcription repression by *Xenopus* ET and its human ortholog TBX3, a gene involved in ulnar-mammary syndrome. Proc Natl Acad Sci USA 96:10212–10217

Hennighausen L, Robinson G (1998) Think globally, act locally: the making of a mouse mammary gland. Genes Dev 12:449–455

Ito A, Asamoto M, Hokaiwado N, Takahashi S, Shirai T (2005) Tbx3 expression is related to apoptosis and cell proliferation in rat bladder both hyperplastic epithelial cells and carcinoma cells. Cancer Lett 219:105–112

Jacobs JJL, Keblusek P, Robanus-Maandag E, Kristel P, Lingbeek M, Nederlof PM, Welsem T van, Vijver MJ van de, Koh EY, Daley GQ, Lohuizen M van (2000) Senescence bypass screen identifies TBX2, which represses Cdkn2a (p19ARF) and is amplified in a subset of human breast cancers. Nat Genet 26:291–299

Jerome L, Papaioannou V (2001) DiGeorge syndrome phenotype in mice mutant for the T-box gene TBX1. Nat Genet 27:286–291

Jerome-Majewska L, Jenkins G, Ernstoff E, Zindy F, Sherr C, Papaioannou V (2005) *Tbx3*, the ulnar-mammary syndrome gene, and *Tbx2* interact in mammary gland development through a p19ARF/p53-independent pathway. Dev Dyn 234:922–933

Jerry DJ, Kuperwasser C, Downing SR, Pinkas J, He C, Dickinson ES, Marconi S, Naber SP (1998) Delayed involution of the mammary epithelium in BALB/c-*p53* null mice. Oncogene 17:2305–2312

Kashuba E, Mattsson K, Klein G, Szekely L (2003) p14ARF induces the relocation of HDM2 and p53 to extranucleolar sites that are targeted by PML bodies and proteasomes. Mol Cancer 5:2–18

Koopman G, Reutelingsperger CPM, Kuijten GAM, Keelmen RMJ, Pals ST, Oers MHJ van (1994) Annexin V for flow cytometric detection of phosphatidylserine expression on B cells undergoing apoptosis. Blood 84:1415–1420

Korgaonkar C, Zhao L, Modestou M, Quelle DE (2002) ARF function does not require p53 stabilization or Mdm2 Relocalization. Mol Cell Biol 22:196–206

Li M, Newbury-Ecob R, Terret J, Wilson D, Curtis A (1997) Holt-Oram syndrome is caused by mutations in TBX5, a member of the brachyury gene family. Nat Genet 15:21–29

Lindsay E, Vitelli F, Su H, Morishima M (2001) TBX1 haploinsufficiency in the DiGeorge syndrome region causes aortic arch defects in mice. Nature 410:97–101

Lingbeek M, Jacobs J, Lohuizen M van (2002) The T-box repressors TBX2 and TBX3 specifically regulate the tumor suppressor gene p14ARF via a variant T-site. J Biol Chem 277:26120–26127

Marcano ACB, Doudney K, Braybrook C, Squires R, Patton MA, Lees MM, Richieri-Costa A, Lidral AC, Murray JC, Moore GE, Stanier P (2004) TBX22 mutations are a frequent cause of cleft palate. J Med Genet 41:68–74

Medina D, Kittrell FS (2003) p53 function is required for hormone-mediated protection of mouse mammary tumorigenesis. Cancer Res 63:6140–6143

Meneghini V, Odent S, Platonova N, Egeo A, Merlo GR (2006) Novel TBX3 mutation data in families with ulnar-mammary syndrome indicate a genotype-phenotype relationship: mutations that do not disrupt the T-domain are associated with less severe limb defects. Eur J Med Genet 49:151–158

Merlo GR, Venesio T, Taverna D, Marte B, Callahan R, Hynes N (1994) Growth suppression of normal mammary epithelial cells by wild-type p53. Oncogene 9:443–453

Merlo G, Fiore L, Basolo F, Duboc L, Hynes N (1995) p53-dependent and p53-independent apoptosis of mammary epithelial cells reveals a role for EGF and insulin as survival factors. J Cell Biol 128:1185–1196

Merlo G, Graus-Porta D, Cella N, Marte B, Taverna D, Hynes N (1996) Growth, differentiation and survival of HC11 mammary epithelial cells: diverse effects of receptor tyrosine kinase-activating growth factors. Eur J Cell Biol 70:97–105

Merscher S, Funke B, Epstein J, Heyer J, Puech A, Lu M (2001) TBX1 is responsible for cardiovascular defects in velo-cardio-facial/DiGeorge syndrome. Cell 104:619–629

Momand J, Zambetti GP (1997) Mdm-2: "big brother" of p53. J Cell Biochem 64:343–352

Morgenstern JP, Land H (1990) Advanced mammalian gene transfer: high titre retroviral vectors with multiple drug selection markers and a complementary helper-free packaging cell line. Nucleic Acids Res 18:3587–3596

Moskowitz IP, Pizard A, Patel VV, Bruneau BG, Kim JB, Kupershmidt S, Roden D, Berul CI, Seidman CE, Seidman JG (2004) The T-box transcription factor Tbx5 is required for the patterning and maturation of the murine cardiac conduction system. Development 131:4107–4116

Naiche L, Papaioannou V (2003) Loss of TBX4 blocks hindlimb development and affects vascularization and fusion of the allantois. Development 130:2681–2693

Normand G, Hemmati PG, Verdoodt B, Haefen C von, Wendt J, Guner D, May E, Dorken B, Daniel PT (2005) p14ARF induces G2 cell cycle arrest in p53- and p21-deficient cells by down-regulating p34cdc2 kinase activity. J Biol Chem 280:7118–7130

Packham E, Brook J (2003) T-box genes in human disorders. Hum Mol Genet 12:R37–R44

Papaioannou V, Silver L (1998) The T-box gene family. BioEssays 20:9–19

Paxton C, Zhao H, Chin Y, Langner K, Reecy J (2002) Murine TBX2 contains domains that activate and repress gene transcription. Gene 283:117–124

Prince S, Carreira S, Vance KW, Abrahams A, Goding CR (2004) TBX2 directly represses the expression of the p21WAF1 cyclin-dependent kinase inhibitor. Cancer Res 64:1669–1674

Resnitzky D, Reed S (1995) Different roles for cyclins D1 and E in regulation of the G1-to-S transition. Mol Cell Biol 15:3463–3469

Rowley M, Grothey E, Couch FJ (2004) The role of TBX2 and TBX3 in mammary development and tumorigenesis. J Mammary Gland Biol Neoplasia 9:109–118

Sherr CJ (1998) Tumor surveillance via the ARF-p53 pathway. Genes Dev 12:2984–2991

Smith J (1999) T-box genes: what they do and how they do it. Trends Genet 15:154–158

Steinman HA, Burstein E, Lengner C, Gosselin J, Pihan G, Duckett CS, Jones SN (2004) An alternative splice form of mdm2 induces p53-independent cell growth and tumorigenesis. J Biol Chem 279:4877–4886

Sugimoto M, Kuo ML, Roussel MF, Sherr CJ (2003) Nucleolar ARF tumor suppressor inhibits ribosomal RNA processing. Mol Cell 11:415–424

Tada M, Smith J (2001) T-targets: clues to understanding the functions of T-box proteins. Dev Growth Differ 43:1–11

Veltmaat J, Maileux A, Thiery J, Bellusci S (2003) Mouse embryonic mammogenesis as a model for the molecular regulation of pattern formation. Differentiation 71:1–17

Visvader JE, Lindeman GJ (2003) Transcriptional regulators in mammary gland development and cancer. Int J Biochem Cell Biol 35:1034–1051

Wang Y, Blandino G, Givol D (1999) Induced p21waf expression in H1299 cell line promotes cell senescence and protects against cytotoxic effect of radiation and doxorubicin. Oncogene 18:2643–2649

Weber JD, Taylor LJ, Roussel MF, Sherr CJ, Bar-Sagi D (1999) Nucleolar ARF sequesters Mdm2 and activates p53. Nat Cell Biol 1:20–26

Weber JD, Jeffers JR, Rehg JE, Randle DH, Lozano G, Roussel MF, Sherr CJ, Zambetti GP (2000) p53-Independent functions of the p19 (ARF) tumor suppressor. Genes Dev 14:2358–2365

Weinstat-Saslow D, Merino M, Manrow R, Lawrence J, Bluth R, Wittenbel K, Simpson J, Page D, Steeg P (1995) Overexpression of cyclin D mRNA distinguishes invasive and in situ breast carcinomas from non-malignant lesions. Nat Med 1:1257–1259

Wilson V, Conlon FL (2002) The T-box family. Genome Biol 3:3008.1–3008.7

Yarbrough WG, Bessho M, Zanation A, Bisi JE, Xiong Y (2002) Human tumor suppressor ARF impedes S-phase progression independent of p53. Cancer Res 62:1171–1177

Yi Y, Shepard A, Kittrell F, Mulac-Jericevic B, Medina D, Said TK (2004) p19ARF determines the balance between normal cell proliferation rate and apoptosis during mammary gland development. Mol Biol Cell 15:2302–2311

Zucchi I, Montagna C, Susani L, Vezzoni P, Dulbecco R (1998) The rat gene homologous to the human gene 9–27 is involved in the development of the mammary gland. Proc Natl Acad Sci USA 95:1079–1084

Zucchi I, Montagna C, Susani L, Montesano R, Affer M, Zanotti S, Redolfi E, Vezzoni P, Dulbecco R (1999) Genetic dissection of dome formation in a mammary cell line: identification of two genes with opposing action. Proc Natl Acad Sci USA 98:13766–13770

Zucchi I, Bini L, Albani D, Valaperta R, Liberatori S, Raggiaschi R, Montagna C, Susani L, Barbieri O, Pallini V, Vezzoni P, Dulbecco R (2002) Dome formation in cell cultures as expression of an early stage of lactogenic differentiation of the mammary gland. Proc Natl Acad Sci USA 99:8660–8665